JOURNAL OF CATALYSIS **161,** 350–358 (1996)
ARTICLE NO. 0192

Dealumination of HZSM-5 Zeolites

II. Methanol to Gasoline Conversion[1]

S. M. Campbell,*,† D. M. Bibby, ‡ J. M. Coddington,* and R. F. Howe§,[2]

*Chemistry Department, University of Auckland, Auckland, New Zealand; ‡Industrial Research Ltd., Petone, New Zealand; §Department of Physical Chemistry, University of New South Wales, Australia; and †Department of Chemistry, Louisiana State University, Shreveport, Louisiana 71105

Received August 21, 1995; revised November 28, 1995; accepted January 31, 1996

Changes in the structure and properties of HZSM-5 zeolites used for extended periods as catalysts in the conversion of methanol to gasoline have been investigated. HZSM-5 samples were characterized using solid-state NMR spectroscopy (^{27}Al and ^{29}Si MAS), infrared spectroscopy; chemical analysis, water and nitrogen adsorption, X-ray diffraction, X-ray photoelectron spectroscopy, and ^{129}Xe NMR spectroscopy of adsorbed xenon. Use of HZSM-5 in methanol conversion was found to cause dealumination of the zeolite lattice. The catalyst lifetime, however, increased after repeated use in MTG cycles. The dealumination is caused by water produced during methanol conversion, although the extralattice aluminum species formed appear to differ from those produced by calcination or mild hydrothermal treatment. The increase in catalyst lifetime is attributed to a decreased rate of coke formation in catalysts containing lower densities of acid sites.

INTRODUCTION

Use of HZSM-5 in fixed bed methanol to gasoline conversion has been found to cause an irreversible loss of catalyst efficiency after a number of conversion–regeneration cycles (1). However, it is not known whether this deactivation results from steaming during conversion or heat treatment during catalyst regeneration.

Few studies of the effects of catalyst use on the structure of HZSM-5 zeolite samples have been reported. In a recent paper by Barrage *et al*. (2) it was concluded, on the basis of ^{29}Si NMR spectra of both fresh and used HZSM-5 samples, that dealumination of the zeolite lattice occurs following catalyst use in the methanol to gasoline conversion reaction. These researchers found that the catalytic behavior of the fresh and "used" catalysts was nearly identical; loss of aluminum from the zeolite lattice appeared to have no detrimental effect on the catalytic activity of the zeolite for methanol conversion.

To pursue this question further, we have taken the HZSM-5 samples utilized in a previous study of the effect on the zeolite structure of calcination and hydrothermal treatment (3) and examined them as MTG catalysts. Repeated conversion–regeneration cycles were carried out to investigate the effect of catalyst aging on catalyst lifetime, activity, and structure for zeolites of different aluminum contents.

EXPERIMENTAL

Methanol Conversion

The HZSM-5 zeolite samples used in this study were those denoted Z12, Z25, and Z74 HZSM-5 in Part I of this study (3). The details of these samples can be found in Table 1 of Part I (3). Samples supplied in the sodium form were cation exchanged three times with 0.5 *M* ammonium nitrate solution to prepare the NH_4ZSM-5 zeolites. Deammonation and activation of the zeolite were carried out in a flow of dry nitrogen, 200 ml min^{-1}, as outlined in Part I (3).

Methanol conversion was carried out in a quartz reactor tube placed in a furnace. Approximately 5 g of NH_4ZSM-5, which had been pressed into small pellets ($3 \times 3 \times 0.5$ mm), was placed in the reactor and held in place by a plug of quartz wool. A relatively wide shallow bed was used to ensure a more homogeneous coking of the zeolite.

Methanol to gasoline conversion was carried out at 648 K using a methanol space velocity of 2.0 g methanol/g zeolite/h. Methanol was introduced into the nitrogen carrier flow, 80 ml min^{-1}, via a needle through a septum into the heated region. In this way the methanol was vaporized and heated to reaction temperature prior to contact with the catalyst. Methanol was pumped into the reactor by a piston driven pump from Fluid Metering Incorporated which had been adapted for low flow rate. The methanol flow rate was adjusted to maintain the methanol space velocity at 2 g/g/h as the mass of zeolite varied between cycles due to removal

[1] This work is dedicated to the memory of Dr. Jan M. Coddington, one of the authors of the paper, who died tragically in May 1992.

[2] To whom correspondence should be addressed at the Department of Physical Chemistry, University of New South Wales, Sydney, NSW 2052, Australia.

0021-9517/96 $18.00

of samples for analysis. The progress of deactivation was followed by monitoring the content of unconverted methanol in the aqueous phase which had been collected in an ice trap at the reactor outlet. The percentage methanol in the aqueous product was determined by means of attenuated total reflectance (ATR)–FTIR spectroscopy, on a Bomem MB-100 instrument at 4 cm^{-1} resolution. The ATR sampling accessory used was a SpectraTech single pass silicon crystal ATR attachment. The ν(CO) stretching vibration mode of methanol at ca. 1000 cm^{-1} was used to determine the methanol concentration, and the method was calibrated with standards of known methanol concentration.

The zeolite was considered to be deactivated when methanol conversion fell to 45%; this point was chosen as that corresponding to cessation of liquid hydrocarbon production during the first cycle with the Z12 HZSM-5 sample.

Before regeneration of the zeolite the system was flushed at 648 K for 2 h with dry nitrogen to remove any residual hydrocarbons. Regeneration gas consisting of 2% oxygen in nitrogen was then fed into the reactor (at 200 ml min^{-1}) as the temperature was raised to 823 K at 2 K min^{-1}. This temperature and the regeneration gas flow was maintained for 24 h to ensure total burn off of coke. A small sample of the regenerated zeolite was removed for characterization following each successive deactivation-regeneration cycle.

A sample of Z25 HZSM-5 was hydrothermally treated under conditions which matched the steam to which the zeolite was subjected during the first four MTG cycles, i.e., a temperature of 648 K, and water introduced at the same molar feed rate as methanol (1 molecule of water is produced for each molecule of methanol converted) and adjusted as necessary to compensate for the decrease in water production as the methanol conversion dropped below 100%. In this way samples exposed to steam for the equivalent of the first four MTG cycles could be compared with samples used for catalysis.

Sample Nomenclature

Used catalyst samples are identified with their corresponding zeolite label, e.g., Z12, Z25, Z74; MTG, to denote catalytic use; and a number indicating the number of deactivation–regeneration cycles the zeolite sample has undergone. For example, Z12MTG3 is a sample of Z12 HZSM-5 zeolite which has been through three MTG deactivation–regeneration cycles. Similarly the analogously steam treated samples are identified with the zeolite label; H_2O, to denote hydrothermal treatment; and a number indicating the number of these analogous "cycles" the zeolite has been subjected to.

Characterization of HZSM-5 Samples

The procedures and instrument parameters used to characterize the samples produced in this work were identical to those used previously (3) with the exception of the ^{29}Si, ^{27}Al MAS NMR spectra which were recorded on a Bruker CXP300 spectrometer and the infrared spectra which were recorded on a Bomem MB-100 FTIR spectrometer operating at 2 cm^{-1} resolution.

RESULTS

Use of HZSM-5 as Catalyst for Methanol to Gasoline Conversion

Figure 1 shows methanol conversion versus time plots for the 2nd, 4th, 7th, 8th, and 10th cycles with the Z25 HZSM-5 sample. The cycle lengths, expressed as the time on stream required for the conversion to fall to 45%, are shown plotted as a function of cycle number in Fig. 2 for HZSM-5 samples of different aluminum content. For each HZSM-5 sample the shortest cycle length was recorded in the first MTG cycle and cycle length increased for each subsequent cycle.

Bulk chemical analyses, for the quantification of silicon and aluminum contents of the used catalysts, were carried out as described in Part I of this study (3). The Si/Al ratios of all samples were the same, within experimental error, as those measured for the parent HZSM-5 sample (3).

XRD patterns and electron micrographs indicated no loss of crystallinity or change in crystallite appearance following use of the zeolite as MTG catalyst.

Solid-State NMR Spectroscopy

Figure 3 shows ^{27}Al MAS NMR spectra of the Z25H parent HZSM-5 and Z25 HZSM-5 zeolite samples used for MTG conversion. The spectra have been scaled for the

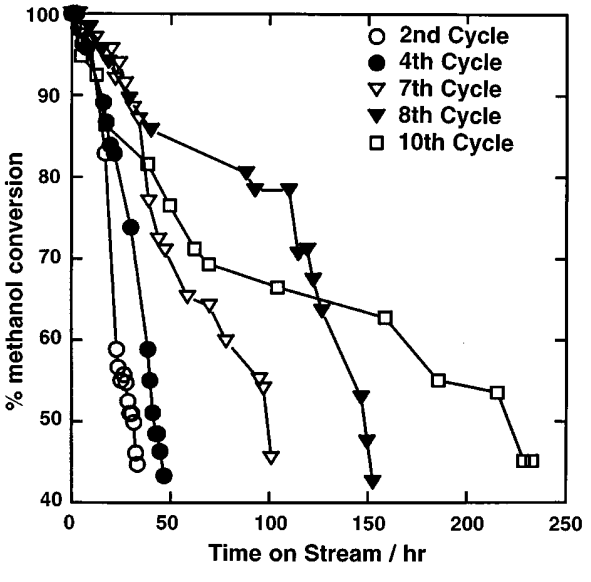

FIG. 1. Percentage methanol conversion over Z25 HZSM-5 as a function of time on stream for selected MTG cycles.

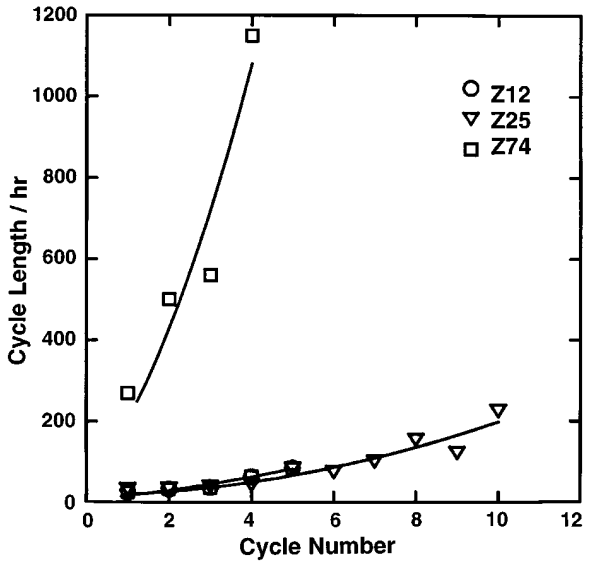

FIG. 2. MTG cycle length as a function of cycle number.

number of scans and sample mass. Several observations can be made from these spectra which also apply to the used Z12 HZSM-5 and Z74 HZSM-5 samples. First, MTG conversion causes loss of signal intensity of the NMR signal at 54 ppm, attributed to tetrahedral lattice aluminum (4). Second, a poorly resolved shoulder at ca. 40 ppm appears after use of the HZSM-5 zeolite as MTG catalyst, which gives the remaining tetrahedral Al signal asymmetric appearance.

The peak area of the NMR signal due to tetrahedral lattice aluminum of each sample, corrected for sample mass and the number of scans taken, was used to quantify the aluminum remaining unperturbed in the zeolite lattice following catalyst use. The results for the used HZSM-5 are given in Table 1, expressed as the number of tetrahedral aluminum atoms per unit cell.

^{27}Al NMR spectra of the Z25 HZSM-5 samples which have been subjected to steam treatment under conditions matching those in MTG cycles, are shown in Fig. 4. The tetrahedral lattice aluminum content measured for the $Z25H_2O$ samples are also shown in Table 1. Over the four cycles for which the analogous steaming was carried out the degree of dealumination was comparable to that following MTG use.

As reported elsewhere (3), adsorption of acetylacetone onto parent Z25H HZSM-5 caused a large decrease in the observed ^{27}Al signal. The tetrahedral signal observed in the ^{27}Al NMR spectra of any of the used samples on which acetylacetone has been adsorbed was less than that observed prior to acetylacetone adsorption. An additional NMR signal at 0 ppm, attributed to octahedral aluminum, was observed in the spectra of all used HZSM-5 upon which acetylacetone had been adsorbed.

^{29}Si MAS NMR spectra of the Z12MTG series of HZSM-5 are shown in Fig. 5. The signal at −105 ppm due to Si(1Al), which was clearly observed in the ^{29}Si NMR spectrum of the Z12H sample, can no longer be seen in the spectra of samples which had been used in MTG conversion. In addition the linewidth of the silicon signal decreased with increasing catalytic use.

Infrared Spectroscopy

Figure 6 shows infrared spectra of the Z25H parent HZSM-5 sample and Z25MTG which have been through the noted number of MTG cycles. The intensity of the infrared band at 3606 cm^{-1} assigned to bridging hydroxyl groups (5) decreases sharply on use of the HZSM-5 as an MTG catalyst. This change is most pronounced after the first cycle; further MTG cycles led to further small losses in the intensity of this band. The 3720 cm^{-1} band due to silanol groups also decreased in intensity after repeated MTG cycles, whereas a broad 3660 cm^{-1} band assigned to extralattice AlOH groups (3) became more clearly visible in used catalysts. Figure 6 also shows the hydroxyl region of the infrared spectra for the $Z25H_2O2$ sample. The intensity of the infrared absorption band at 3606 cm^{-1}, decreased in the same manner, and to a similar degree, as was observed for the samples used in the MTG reaction.

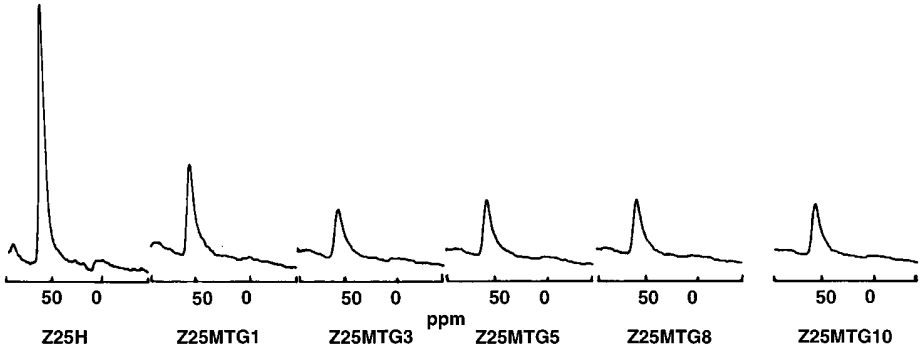

FIG. 3. ^{27}Al MAS NMR spectra of selected samples from the Z25MTG series.

TABLE 1

Characterization of HZSM-5 Samples Used in the Conversion of Methanol to Gasoline

HZSM-5 sample	Lattice Al content (NMR) (Al (uc)$^{-1}$)	Extralattice content (NMR) (Al (uc)$^{-1}$, ±0.5)	Bridging OH conc. (IR studies) ((uc)$^{-1}$, ±0.4)	Brønsted acid conc. (py[a] ads.) ((uc)$^{-1}$, ±0.2)	Lewis acid conc. (py[a] ads.) ((uc)$^{-1}$, ±0.2)	Lattice Al content (framework IR) (Al (uc)$^{-1}$, ±1.0)	Pore volume (from N_2 isotherm) (cm^3 g^{-1}, ±3%)	Si/Al$_{surf}$ (XPS)	^{129}Xe NMR chemical shift at zero coverage (ppm, ± 1.5)	Lattice Al content (^{129}Xe NMR) (Al(uc)$^{-1}$, ± 1.0)
Z12H	7.2 ± 0.4	0.4	7.4	7.3	0.5	7.5	105	14 ± 2	114	7.5
Z12MTG1	1.5 ± 0.3	5.7	3.4	2.1	1.0	1.9	94	9 ± 1	110	4.2
Z12MTG2	1.4 ± 0.3	5.8	1.3	1.5	1.0	1.3	88	—	—	—
Z12MTG3	0.9 ± 0.2	6.3	0.8	1.2	0.5	1.3	90	9 ± 1	109	3.9
Z12MTG4	0.8 ± 0.2	6.4	0.6	0.9	0.4	1.2	86	—	—	—
Z12MTG5	0.5 ± 0.2	6.7	—	0.6	0.4	0.7	84	7 ± 1	106	2.6
Z25H	3.7 ± 0.1	—	3.7	3.5	0.2	3.7	90	23 ± 5	—	—
Z25MTG1	1.2 ± 0.3	2.5	0.9	1.6	0.4	1.8	85	28 ± 5	—	—
Z25MTG2	0.9 ± 0.3	2.8	0.7	1.1	0.3	1.7	80	—	—	—
Z25MTG3	0.7 ± 0.3	3.0	0.5	0.9	0.9	1.2	78	17 ± 2	—	—
Z25MTG4	0.7 ± 0.3	3.0	0.4	0.9	0.4	1.2	83	—	—	—
Z25MTG5	0.8 ± 0.3	2.9	0.2	0.8	0.3	1.1	81	—	—	—
Z25MTG6	0.7 ± 0.3	3.0	0.6	0.8	1.1	1.2	76	16 ± 2	—	—
Z25MTG7	0.7 ± 0.3	3.0	0.3	0.7	0.5	1.2	82	—	—	—
Z25MTG8	0.7 ± 0.3	3.0	0.5	0.8	0.9	1.2	79	17 ± 2	—	—
Z25MTG9	0.7 ± 0.3	3.0	0.6	0.7	0.4	1.4	73	—	—	—
Z25MTG10	0.7 ± 0.3	3.0	0.7	0.8	0.3	1.0	72	16 ± 2	—	—
Z25H$_2$O1	0.7 ± 0.3	2.8	0.9	1.0	0.4	2.1	84	18 ± 2	—	—
Z25H$_2$O2	0.9 ± 0.3	2.8	0.9	0.9	0.2	1.8	82	—	—	—
Z25H$_2$O3	0.9 ± 0.3	2.7	1.0	1.0	0.2	1.4	84	16 ± 2	—	—
Z25H$_2$O4	0.7 ± 0.3	2.8	0.9	1.0	0.3	1.4	83	—	—	—
Z74H	1.3 ± 0.1	0.0	1.2	1.1	0.1	1.2	117	—	—	—
Z74MTG1	0.5 ± 0.1	0.8	0.5	0.6	0.3	0.7	102	—	—	—
Z74MTG2	0.4 ± 0.1	0.9	0.4	0.4	0.2	0.7	99	—	—	—
Z74MTG3	0.3 ± 0.1	1.0	—	0.4	0.1	0.5	98	—	—	—
Z74MTG4	0.3 ± 0.1	1.0	—	0.4	0.5	0.3	97	3.8 ± 4.0	—	—

[a] py, pyridine.

Quantification of the hydroxyl concentration was carried out by measurement of the peak area of the absorption band at 3606 cm^{-1}. Peak areas were corrected for wafer thickness using the peak areas of the framework overtone bands. The measured peak areas are presented in Table 1 as hydroxyl sites per unit cell for all used HZSM-5 samples. Within experimental error, the loss of hydroxyl groups observed for the Z25H$_2$O samples was the same as that seen for samples used in the corresponding number of MTG cycles.

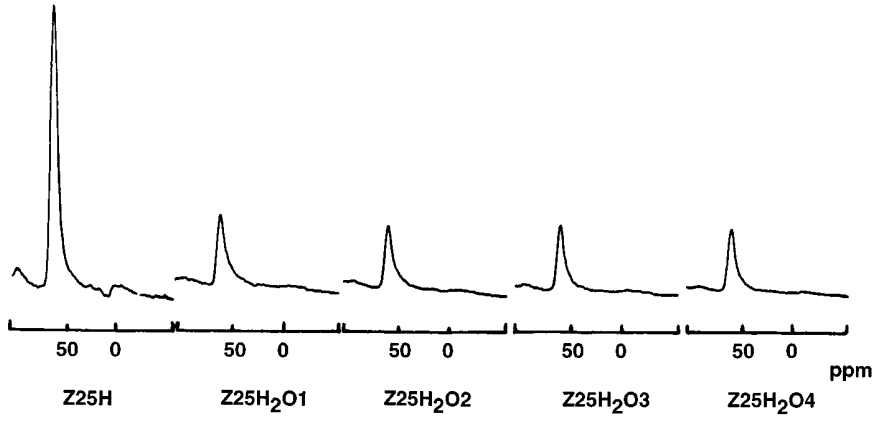

FIG. 4. ^{27}Al MAS NMR spectra of HZSM-5 hydrothermally treated to match conditions occurring in MTG conversion.

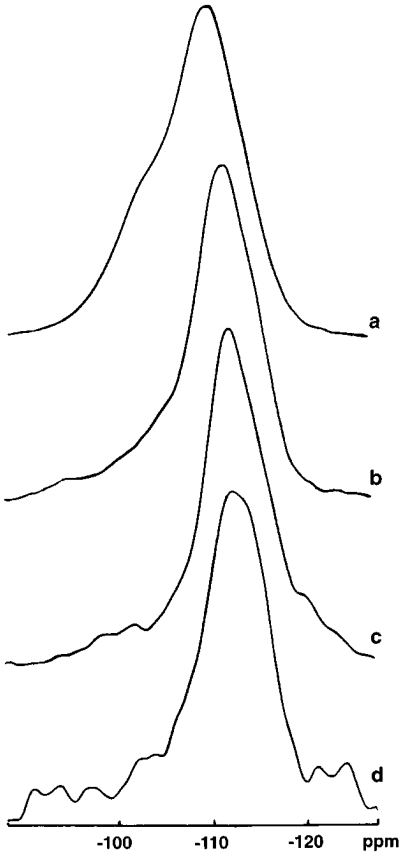

FIG. 5. ^{29}Si MAS NMR spectra of Z12 HZSM-5 used in MTG conversion: (a) Z12H, (b) Z12MTG1, (c) Z12MTG3, (d) Z12MTG5.

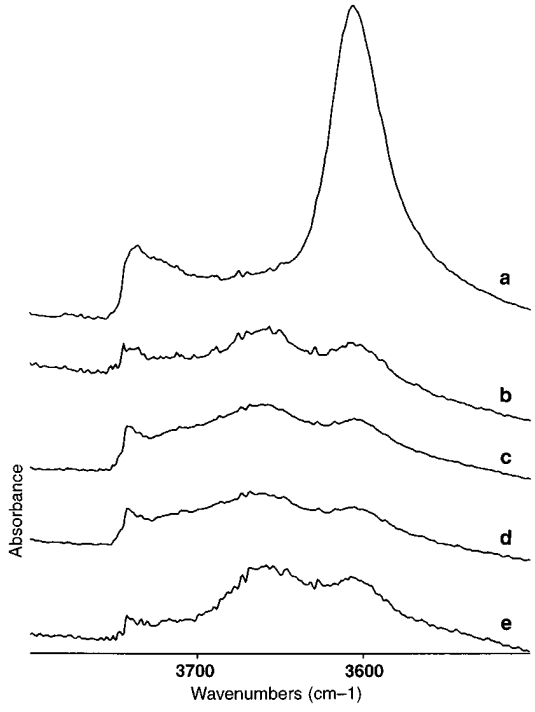

FIG. 6. Infrared spectra of selected used and hydrothermally treated Z25 HZSM-5 samples: (a) Z25H, (b) Z25MTG2, (c) Z25MTG6, (d) Z25MTG8, (e) Z25H_2O2.

Pyridine was adsorbed onto the used HZSM-5 MTG samples as described under Experimental in Part I (3). Subtraction spectra, showing the infrared absorption bands due to pyridine adsorbed on various Z25MTG and Z25H_2O used HZSM-5 samples, are presented in Fig. 7. The intensity of the band at 1543 cm^{-1}, due to pyridine adsorbed on Brønsted acid sites (6), decreased markedly following use of HZSM-5 for MTG conversion. Brønsted acid site concentrations of the HZSM-5 samples in the Z25MTG series were determined by measurement of peak area of this infrared band at 1543 cm^{-1}, corrected for wafer thickness (Table 1). Bridging hydroxyl group concentrations and Brønsted acid site concentrations were found to be the same within experimental error.

Table 1 shows both the Brønsted and Lewis acid site concentrations of the used and steam-treated HZSM-5 samples calculated from the peak areas of the infrared bands at 1543 and 1454 cm^{-1}, respectively, taking into account the absorptivity values of the two IR bands (6) and variations in wafer thickness. Similar concentrations of Lewis acid sites were observed following use of HZSM-5 as MTG catalyst as in the corresponding hydrothermal treatment.

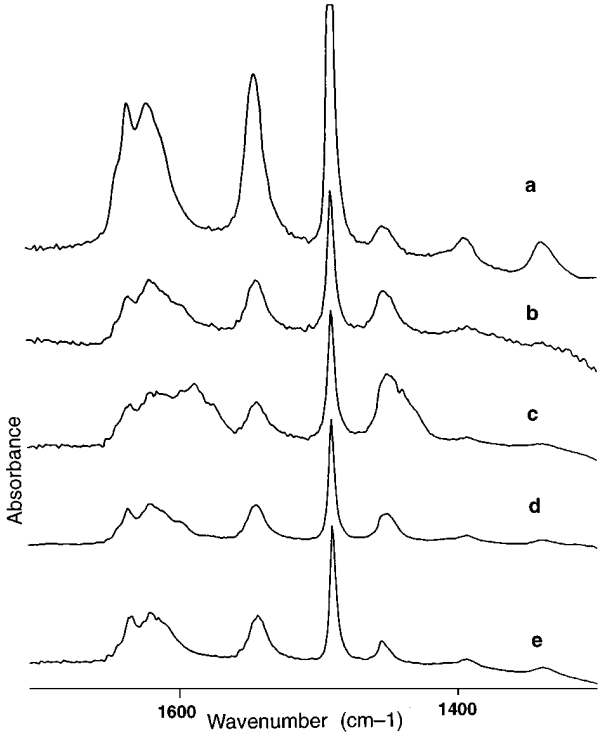

FIG. 7. Infrared spectra of pyridine adsorbed on selected used and hydrothermally treated Z25 HZSM-5 samples: (a) Z25H, (b) Z25MTG2, (c) Z25MTG6, (d) Z25MTG8, (e) Z25H_2O2.

It was concluded in Part I (3) that the frequencies of the strong vibrational modes, observed between 400 and 1200 cm^{-1} in the infrared spectra, show a dependence on the aluminum content of the zeolite and therefore can be used to determine the framework aluminum content of dealuminated HZSM-5 samples. The plots of band frequency as a function of lattice aluminum content for parent HZSM-5 (Fig. 6 of Part I (3)) were used to calculate lattice aluminum contents of the HZSM-5 samples used for MTG conversion. Table 1 shows the lattice aluminum contents determined in this way from the frequencies of the framework vibrational modes.

Nitrogen Adsorption Isotherms

The adsorption isotherms of nitrogen at 77 K were recorded for both parent and used HZSM-5 catalysts. Use of HZSM-5 led to a loss in the volume of nitrogen adsorbed at any given nitrogen pressure, corresponding to a decrease in the pore volume of the zeolite sample. As previously (3), the pore volume of each of the HZSM-5 samples was taken as the volume at STP of nitrogen adsorbed at a nitrogen pressure of $P/P_s = 0.2$. Pore volumes calculated in this way are given in Table 1.

Adsorption of Water

The quantity of water adsorbed in the zeolite samples following equilibration at 80% relative humidity was determined for the used MTG samples. The water contents per gram of dry zeolite of the Z25MTG HZSM-5 samples are given as a function of lattice aluminum content in Fig. 8 together with the results obtained for parent HZSM-5 samples. The quantity of water adsorbed in the used HZSM-5 samples decreased, as the number of cycles increased, even when the lattice aluminum content remained constant between consecutive MTG cycles. Results from the $Z25H_2O$ samples are also shown in Fig. 8. These four samples also showed a fall in water content following each "cycle" despite the observation that the degree of dealumination, and therefore the extralattice aluminum content, remained constant.

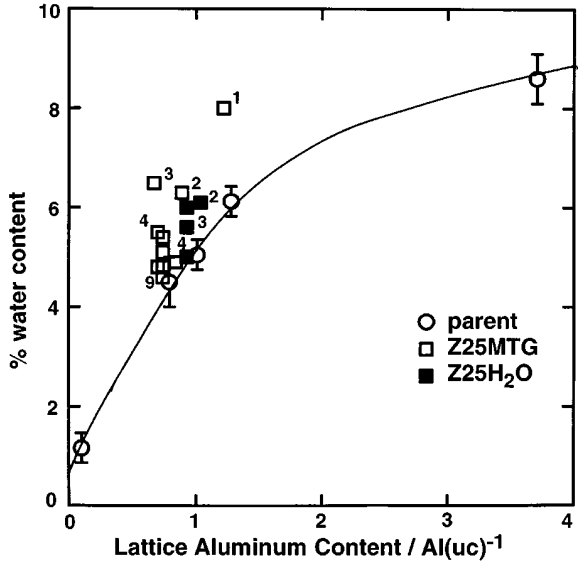

FIG. 8. Water contents of HZSM-5 as parent, used for MTG conversion, and analogously steamed, as a function of lattice aluminum content. Number labels on plotted points indicate the number of cycles.

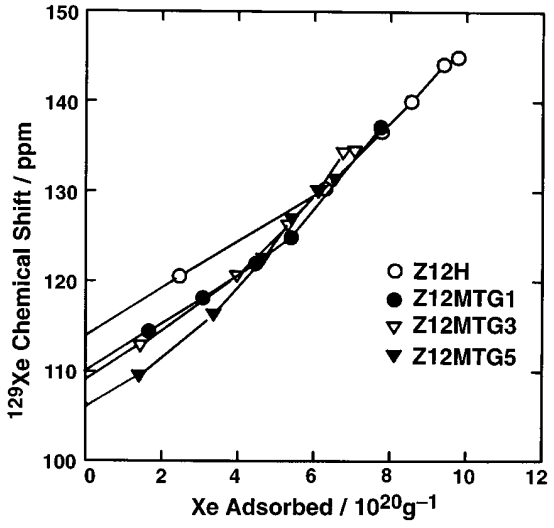

FIG. 9. ^{129}Xe chemical shift of xenon adsorbed on selected used HZSM-5 samples as a function of the quantity of xenon adsorbed.

X-Ray Photoelectron Spectroscopy

XPS spectra were recorded for HZSM-5 samples used for MTG conversion and surface Si/Al ratios (Si/Al_{surf}) calculated (Table 1). Use of the HZSM-5 for MTG conversion led to enrichment of aluminum on the surface of the zeolite. This enrichment occurred during the first cycle for the Z12 MTG series but only after the first cycle for the Z25 HZSM-5 sample. Surface Si/Al ratios calculated for the Z25MTG3–MTG10 samples were the same within experimental error.

^{129}Xe NMR Spectroscopy of Adsorbed Xenon

Measurement of the ^{129}Xe chemical shift as a function of the xenon adsorbed in the zeolite was performed as described in Part I (3). ^{129}Xe chemical shifts plotted as a function of xenon adsorbed in the zeolite for the Z12MTG1, Z12MTG3, and Z12MTG5 HZSM-5 samples are shown in Fig. 9. The gradients of these plots increased with increasing catalytic use. Values of the chemical shift extrapolated to zero xenon coverage for the Z12MTG HZSM-5 samples, determined as described in Part I (3), are given in Table 1. The intercept value decreased with the number of cycles of MTG conversion. The apparent aluminum contents of the

used HZSM-5 were calculated from the measured values of chemical shift at zero xenon using previously published data (7). These apparent lattice aluminum contents are shown in Table 1.

DISCUSSION

Use of HZSM-5 in Methanol Conversion

In the shallow catalyst bed used here methanol conversion was less than 100% (typically ca. 98%), even at the beginning of a cycle. However, the methanol conversion was maintained at a high level over half the total cycle length, after which the decrease in conversion became progressively larger. The cycle lengths observed for conversion using the Z12 and Z25 HZSM-5 samples were short compared to those of Z74 HZSM-5 and those reported by Yurchak *et al.* (8). The length of the first cycle in the Mobil Study was reported as 15 days or 600 g of methanol converted per gram of catalyst. A study by Aldridge *et al.* (9) found that there was a large variation in the length of cycle for different HZSM-5 samples. In particular the first cycle length for a number of the samples was less than or equal to 24 h and it was noted that the cycle length was short for samples of high aluminum content similar to that of the Z12 and Z25 HZSM-5 samples used in this study.

In the present study, in the aging study carried out by Mobil Research Laboratories (8), and also in commercial production at the Synfuels Plant, New Zealand (10), the first cycle was the shortest cycle. However, the exponential increase in cycle length observed in this study (Fig. 2) was not seen in the Mobil data (8) or in the commercial production (10). In the Mobil Study (8) the cycle lengths for cycles 3 through 5 are only slightly higher than the first cycle, while the length of cycle appears to stabilize above cycle 5 at a value greater than 21 days, each cycle involving the processing of 800 g of methanol per gram of zeolite. Repeated cycling of the samples used here, regardless of the aluminum content of the zeolite sample, produced a catalyst which was more resistant to coke deactivation, but which still behaved as an efficient methanol to gasoline catalyst. Bibby (11) found that coke content in deactivated HZSM-5 decreased in later cycles. It was concluded that this was indicative of permanent loss of acid sites with cycling. However, it was observed that this loss did not impair catalyst lifetime.

The dramatically longer catalyst lifetimes observed with Z74 warrant comment. This zeolite has a higher silicon : aluminum ratio than the other two, but the lifetime of the fresh Z74 catalyst is still much longer than that of the Z12 and Z25 zeolites after repeated cycling (which have comparable lattice silicon : aluminum ratios). A referee has suggested that the enhanced lifetimes of Z74 may be due to crystal size effects; this suggestion is commented on below.

Effect of MTG Conversion on the HZSM-5 Lattice Structure

As was also observed in Part I (3) for the HZSM-5 samples which had been calcined and hydrothermally treated, use of the HZSM-5 as an MTG catalyst caused loss of total ^{27}Al NMR signal. Bulk chemical analysis showed that no loss of aluminum from the zeolite bulk occurred. Similarly, in a study conducted by Aukett *et al.* (12) on the use of HZSM-5 as catalyst for the alkylation of benzene, it was reported that no loss of total aluminum content occurred. The loss of NMR signal is therefore attributed to the formation of aluminum species of less than cubic symmetry, as described in Part I (3). The presence of these "NMR invisible" aluminum species in the samples was confirmed by the partial visualization of this low symmetry aluminum species with acetylacetone.

The loss of the signal at −105 ppm in the ^{29}Si MAS NMR spectra (Fig. 5), corresponding to Si(1Al), indicated that the Si–O–Al bonds in the zeolite lattice had been broken and confirmed the loss of aluminum from the zeolite lattice during MTG conversion. In addition, the linewidth of the silicon signal was observed to decrease with increasing catalytic use. This narrowing of the signal is also symptomatic of loss of aluminum from the zeolite lattice. Lattice aluminum contents of the HZSM-5 samples used in MTG reactions determined from the frequencies of the framework vibrational modes (3) compared favorably with the values for lattice aluminum content determined from the NMR studies.

Brønsted acid site concentrations, as measured from the intensities of the infrared adsorption band of pyridinium at 1543 cm^{-1} following adsorption of pyridine; bridging hydroxyl concentrations, as measured from the infrared absorption band at 3606 cm^{-1} in the spectra; and lattice aluminum contents calculated from ^{27}Al NMR were the same within experimental error for each of the used HZSM-5 samples (Table 1). The conclusion from Part I (3), that dealumination of the zeolite by calcination or hydrothermal treatment was associated with an equivalent loss of bridging hydroxyl group concentration and Brønsted acidity, also applies for dealumination of HZSM-5 through use in MTG conversion.

For each of the HZSM-5 samples of different aluminum content the same observations are made; following the first MTG cycle the lattice aluminum content of the zeolite dropped to about 30% of that observed for parent HZSM-5. On repeated use of the HZSM-5 zeolite in successive MTG cycles very little further dealumination occurred: the lattice aluminum content appeared to reach an equilibrium value after a small number of MTG cycles.

A number of researchers (13) have observed that the degree of dealumination of zeolite materials following steam treatment was dependent on the temperature at which the treatment was carried out. Higher temperatures

led to a higher degree of dealumination of the zeolite lattice.

Considering the low temperature at which the MTG conversion (648 K) and the regeneration (823 K) were carried out, the extent of dealumination during a single MTG cycle was high in comparison with that observed following calcination or hydrothermal treatments carried out at considerably higher temperatures as outlined in Part I (3). The close similarities in dealumination extent between the MTG samples and those subjected to hydrothermal treatment under MTG conditions for similar periods of time indicate, however, that dealumination is due to the presence of water under MTG conditions, and not for instance to the presence of organic acids during MTG (14) or to local high temperatures generated during regeneration between cycles. The water vapor pressure of ca. 350 Torr during MTG and the duration of the MTG cycles both encourage dealumination. These findings are consistent with the results of Brunner *et al.* (15), who studied the effect of a mild hydrothermal treatment on the aluminum in HZSM-5 for a range of water vapor pressures. The degree of dealumination was shown in their work to be strongly dependent on the water vapor pressure at pressures below 150 Torr, and relatively constant at higher pressures.

It is significant that, despite the loss of up to ca. 90% of the lattice aluminum atoms, and therefore loss of what are considered to be the active catalytic sites (16), the HZSM-5 samples continue to perform well as MTG catalysts. In fact, the used zeolite samples are better catalysts than fresh samples, as evidenced by the increase in quantity of methanol converted before deactivation.

Efficient MTG catalysis requires only a very small number of lattice aluminum in the zeolite. This is an extension of the earlier observation that a lower aluminum content HZSM-5 sample has a considerably longer catalytic lifetime than HZSM-5 of higher aluminum content and is in agreement with the suggestion (16) that only one aluminum in as many as 1000 may be required to account for the activity of HZSM-5. The density of acid sites will, however, exert a strong influence of coke forming reactions, particularly intermolecular hydrogen transfer (17), so that overall catalyst performance is improved when the number of acid sites is decreased. Coke formation in methanol conversion has been shown to occur in two stages: initial formation of internal coke poisoning acid sites within the zeolite pores, followed by coke deposition on the external surface. It is only during this latter stage of coke formation that methanol conversion is completely suppressed (17). The lower external surface area of zeolite Z74 may thus account for the longer catalyst lifetimes observed with this zeolite, although we note that further experiments with a series of zeolites having identical lattice aluminum contents but different crystal sizes are needed to confirm this suggestion.

Extralattice Aluminum

The catalyst lifetime continued to increase in successive MTG cycles when no further changes in the active site concentrations were observed. Other changes affecting coke formation must therefore also occur. We suggest that these changes involve the extralattice aluminum species formed on hydrothermal dealumination during MTG cycles.

Very little octahedral aluminum was observed in the ^{27}Al NMR spectra of MTG used samples, in contrast with those, of the hydrothermally treated HZSM-5 samples in Part I (3). Small amounts of octahedral aluminum formed during the deammonation of the zeolite was not affected by calcination or mild hydrothermal treatment (3) but was almost completely lost during a single MTG cycle or during hydrothermal treatment under the same conditions as an MTG cycle. This suggests that the extralattice aluminum species formed following prolonged catalyst use may differ from that formed as a result of calcination or mild hydrothermal treatment (3) and, as the observation was made for both used and analogously steamed HZSM-5, that these differences are due to the effect of the higher vapor pressure of water and the longer duration of the treatment.

Only a small number of Lewis acid sites were observed following use of HZSM-5 for MTG conversion, or following analogous steam treatment. Lewis acid site concentrations determined for the used and analogously steamed Z25 HZSM-5 are comparable to those measured in Part I (3). For all samples, the Lewis acid site concentration was low in comparison with the extralattice aluminum content.

It was found that the quantity of water adsorbed by Z25 (Fig. 8) decreased as the number of cycles increased, even for cycles 3 through 10 where the lattice and extralattice aluminum contents remained constant. Following the first three cycles, Z25MTG1–MTG3, the adsorption of water was in excess of that associated with the lattice aluminum. However, the water content continued to fall and after 9 or 10 MTG cycles fell upon the line in Fig. 8 describing the percentage water content in HZSM-5 samples containing no extralattice aluminum. The decrease in the water content is attributed to the extralattice aluminum species becoming less hydrophilic with increasing time on stream in MTG.

The pore volume loss observed following the early cycles was comparable to that observed for calcined or hydrothermally treated samples (3) of a similar degree of dealumination. However, the pore volume continued to decrease in later MTG cycles when no corresponding observable increase in extralattice aluminum content occurred (Table 1). Migration and aggregation of extralattice aluminum species to form larger clusters which close off areas of the pore structure for nitrogen adsorption would account for these observations.

Use of the HZSM-5 as an MTG catalyst led to enrichment of aluminum on the surface of the zeolite, as measured by XPS. The Si : Al ratios did not continue to increase,

however, with increasing cycle number; limiting values were reached after 3 or 4 cycles (Table 1). There is evidently not an ongoing process of migration of aluminum to the external surface.

As illustrated in Fig. 9, the gradients of plots of xenon chemical shift versus coverage increased with increasing MTG cycle number. These changes are consistent with the nitrogen pore volume data indicating progressive loss of pore volume. Loss of aluminum from the zeolite lattice also reduces the xenon chemical shift at zero coverage. However, values for the lattice aluminum content of used samples, as determined from the ^{129}Xe chemical shift, are consistently higher than the values of lattice aluminum content determined from NMR and infrared studies. As was concluded in Part I (3), the presence of extralattice aluminum in the zeolite pores also contributes to the electric field which determines the xenon chemical shift at zero coverage. The contribution of extralattice aluminum to the electric field experienced by adsorbed xenon in these samples, which have been used in MTG conversion, confirms that the extralattice aluminum is largely remaining in the pores of the zeolite.

CONCLUSIONS

This work has shown that extensive dealumination of the ZSM-5 lattice occurs during the MTG reaction and that this is caused by the high water vapor pressures present. Despite the loss of up to 90% of the lattice aluminum, the used catalysts showed enhanced performance in terms of the total quantity of methanol converted before deactivation. Coking occurred more slowly on used catalyst and catalytic lifetimes increased dramatically for all three samples of different aluminum content used. This confirms that only a small active site concentration is necessary for HZSM-5 to be an efficient and effective MTG catalyst. The density of acid sites clearly influenced strongly the coke forming reactions.

The catalyst lifetimes continued to increase when no further measurable dealumination of the HZSM-5 was occurring, indicating that changes in the nature of the extralattice aluminum species also affect coke formation. These changes appear to involve migration and aggregation of aluminum species during prolonged MTG cycling, although the detailed chemistry remains uncertain. The implications of these findings for working catalysts are important. An HZSM-5 catalyst of low aluminum content will be a superior working catalyst in terms of the quantity of methanol converted before deactivation, and higher aluminum content HZSM-5 can be improved by pretreatment which dealuminates the zeolite lattice and modifies the extralattice aluminum species present.

ACKNOWLEDGMENTS

This work was supported in part by funding from the New Zealand Department of Scientific and Industrial Research (now Industrial Research Ltd). We thank also CSIRO, Division of Coal and Energy Technology, North Ryde, for the use of NMR instrumentation and Dr. T. Vassallo for assistance with the NMR measurements.

REFERENCES

1. Schipper, P. H., and Krambeck, F. J., *Chem. Eng. Sci.* **41**, 1013 (1986).
2. Barrage, M. C., Bauer, F., Ernst, H., Fraissard, J. P., Freude, D., and Pfeifer, H., *Catal. Lett.* **6**, 201 (1990).
3. Campbell, S. M., Bibby, D. M., Coddington, J. M., Howe, R. F., and Meinhold, R. M., *J. Catal.,* in press.
4. Fyfe, C. A., Gobbi, G. C., Hartman, J. S., Klinowski, J., and Thomas, J. M., *J. Phys. Chem.* **86**, 1247 (1982).
5. Topsoe, N. Y., Pedersen, K., and Derouane, E. G., *J. Catal.* **70**, 41 (1981).
6. Datka, J., *J. Chem. Soc. Faraday Trans.* **77**, 2877 (1981).
7. Alexander, S. M., Coddington, J. M., and Howe, R. F., *Zeolites* **11**, 368 (1991).
8. Yurchak, S., Voltz, S. E., and Warner, J. P., *Ind. Eng. Chem. Process Des. Dev.* **18**, 527 (1979).
9. Aldridge, L. P., Bibby, D. M., and Milestone, N. B., *N.Z. J. Technol.* **1**, 163 (1985).
10. Allum, K. G., and Williams, A. R., *in* "Studies in Surface Science and Catalysis" (D. M. Bibby, *et al.*, Eds.), Vol. 36, p. 691. Elsevier, Amsterdam, 1988.
11. Bibby, D. M., Poster abstract, 7th International Zeolite Conference, "New Developments in Zeolite Science and Technology," Tokyo, Japan, August 17–22, 1986.
12. Aukett, P. N., Cartlidge, S., Poplett, I. J. F., *Zeolites* **6**, 169 (1986).
13. (a) Freude, D., Frohlich, T., Pfeifer, H., and Scheler, G., *Zeolites* **3**, 171 (1983). (b) Engelhardt, G., Lohse, U., Samoson, A., Magi, M., Tarmak, M., and Lippmaa, E., *Zeolites* **2**, 59 (1982). (c) Engelhardt, G., Lohse, U., Patzelova, V., Magi, M., and Lippmaa, E., *Zeolites* **3**, 233 (1983).
14. Personal communication, Synfuels Engineers, New Plymouth, New Zealand, August 1990.
15. Brunner, E., Ernst, H., Freude, D., Frohlich, T., Hunger, M., and Pfeifer, H., *J. Catal.* **127**, 34 (1991).
16. Haag, W. O., Lago, R. M., and Weisz, P. B., *Nature* **309**, 589 (1984).
17. Bibby, D. M., Howe, R. F., and McClellan, G. D., *Appl. Catal.* **93**, 1 (1992).